

2008

# Probing thickness-dependent dislocation storage in freestanding Cu films using residual electrical resistivity

Shakti Singh Chauhan  
*Iowa State University, shakti@iastate.edu*

Ashraf F. Bastawros  
*Iowa State University, bastaw@iastate.edu*

Follow this and additional works at: [http://lib.dr.iastate.edu/aere\\_pubs](http://lib.dr.iastate.edu/aere_pubs)

 Part of the [Aerospace Engineering Commons](#)

The complete bibliographic information for this item can be found at [http://lib.dr.iastate.edu/aere\\_pubs/67](http://lib.dr.iastate.edu/aere_pubs/67). For information on how to cite this item, please visit <http://lib.dr.iastate.edu/howtocite.html>.

---

This Article is brought to you for free and open access by the Aerospace Engineering at Iowa State University Digital Repository. It has been accepted for inclusion in Aerospace Engineering Publications by an authorized administrator of Iowa State University Digital Repository. For more information, please contact [digirep@iastate.edu](mailto:digirep@iastate.edu).

---

# Probing thickness-dependent dislocation storage in freestanding Cu films using residual electrical resistivity

## Abstract

Residual electrical resistivity measurement is employed to study dislocation storage under tensile loading of freestanding electroplated Cu films (1–5 μm grain size and 2–50 μm thickness). The results indicate that the nature of thickness effects (strengthening or weakening) depends on the underlying deformation mechanisms via the average grain size. A threshold grain size of about  $d_g = 5 \mu\text{m}$  is identified to distinguish grain size effects in thicker films from those in thinner films. For  $d_g > 5 \mu\text{m}$ , diminishing microstructural constraint with reduced thickness weakens the films due to dislocation annihilation near the free surface. For  $d_g < 5 \mu\text{m}$ , reduction of film thickness leads to strengthening via grain boundary-source starvation.

## Keywords

Copper alloys, Copper plating, Crystal growth, Electric resistance, Grain boundaries, Grain size and shape, metallic films, molecular beam epitaxy, deformation mechanisms, dislocation annihilation

## Disciplines

Aerospace Engineering

## Comments

The following article appeared in *Applied Physics Letters* 93 (2008): 041901 and may be found at doi: [10.1063/1.2961006](https://doi.org/10.1063/1.2961006).

## Rights

Copyright 2008 American Institute of Physics. This article may be downloaded for personal use only. Any other use requires prior permission of the author and the American Institute of Physics.

## Probing thickness-dependent dislocation storage in freestanding Cu films using residual electrical resistivity

Shakti Chauhan and Ashraf F. Bastawros

Citation: [Applied Physics Letters](#) **93**, 041901 (2008); doi: 10.1063/1.2961006

View online: <http://dx.doi.org/10.1063/1.2961006>

View Table of Contents: <http://scitation.aip.org/content/aip/journal/apl/93/4?ver=pdfcov>

Published by the [AIP Publishing](#)

---

### Articles you may be interested in

[Significant enhancement of the strength-to-resistivity ratio by nanotwins in epitaxial Cu films](#)

[J. Appl. Phys.](#) **106**, 024313 (2009); 10.1063/1.3176483

[Indentation size dependent plastic deformation of nanocrystalline and ultrafine grain Cu films at nanoscale](#)

[J. Appl. Phys.](#) **105**, 083521 (2009); 10.1063/1.3110087

[Classical size effect in oxide-encapsulated Cu thin films: Impact of grain boundaries versus surfaces on resistivity](#)

[J. Vac. Sci. Technol. A](#) **26**, 605 (2008); 10.1116/1.2938395

[Electrical resistivity of Cu films deposited by ion beam deposition: Effects of grain size, impurities, and morphological defect](#)

[J. Appl. Phys.](#) **99**, 094909 (2006); 10.1063/1.2194247

[Characterization of electroplated copper films for three-dimensional advanced packaging](#)

[J. Vac. Sci. Technol. B](#) **22**, 1108 (2004); 10.1116/1.175217

---

The advertisement features a white Lake Shore Model 372 cryogenic temperature controller on the left, with a digital display showing '98.837'. To its right is a detailed view of a cryogenic system with various components like coils and pipes. The Lake Shore CRYOTRONICS logo is in the top right corner.

Precise temperature control  
for **cryogenic research**

**Model 372**

Lake Shore  
CRYOTRONICS

# Probing thickness-dependent dislocation storage in freestanding Cu films using residual electrical resistivity

Shakti Chauhan and Ashraf F. Bastawros<sup>a)</sup>

Department of Aerospace Engineering, Iowa State University, Ames, Iowa 50011 USA

(Received 20 November 2007; accepted 1 July 2008; published online 28 July 2008)

Residual electrical resistivity measurement is employed to study dislocation storage under tensile loading of freestanding electroplated Cu films (1–5  $\mu\text{m}$  grain size and 2–50  $\mu\text{m}$  thickness). The results indicate that the nature of thickness effects (strengthening or weakening) depends on the underlying deformation mechanisms via the average grain size. A threshold grain size of about  $d_g = 5 \mu\text{m}$  is identified to distinguish grain size effects in thicker films from those in thinner films. For  $d_g > 5 \mu\text{m}$ , diminishing microstructural constraint with reduced thickness weakens the films due to dislocation annihilation near the free surface. For  $d_g < 5 \mu\text{m}$ , reduction of film thickness leads to strengthening via grain boundary-source starvation. © 2008 American Institute of Physics.

[DOI: 10.1063/1.2961006]

The structural miniaturization, driven primarily by applications involving microelectronics and microelectromechanical systems, has led many experimental<sup>1–7</sup> and computational<sup>8,9</sup> studies to focus on the physical mechanisms responsible for size effects in metallic thin films. Two contrasting size-dependent responses have been reported in the literature for the tensile behavior of freestanding films. For films with thickness  $t$  and grain size  $d_g$  in the micron to submicron range, film strength is observed to increase with a reduction in film thickness at a constant grain size.<sup>3</sup> By contrast, for  $t$  and  $d_g \sim O(10\text{--}100 \mu\text{m})$  in both bulk and foil-type specimens, a weakening effect has been reported when reducing film thickness at a constant grain size.<sup>10–12</sup>

This work addresses the increases in film yield strength attendant upon reductions in film thickness for freestanding films with small grains ( $d_g = 1\text{--}5 \mu\text{m}$ ) and film thicknesses ( $t = 2\text{--}50 \mu\text{m}$ ) to provide thickness-to-grain-size ratios of  $\lambda = 0.5\text{--}30$ . Residual electrical resistivity measurements (RERMs) were conducted on the films both before and after deformation to elucidate their microstructural bases, as well as any underlying deformation mechanisms leading to the observed size effects. The transition from film thickness-dependent weakening to strengthening with reductions in grain size was also addressed with regard to the identified deformation mechanisms.

The Cu films were produced using a pulsed electrodeposition method. A peak current density of 250 mA/cm<sup>2</sup> with a 400 ms pulse and 1% duty cycle was employed to yield Cu

films with  $d_g \sim 200 \text{ nm}$  and an average relative density of 99.83%. The films were deposited on microscopic glass slides with a 50 nm sputtered Cu seed layer. The deposited film was patterned and subsequently released using a photolithographic lift-off technique to obtain a freestanding tensile “dog-bone” specimen of 5 mm gauge length and 1 mm width. The films as deposited were further annealed at 400, 500, and 600 °C for 1 h in a nitrogen environment to yield average  $d_g$  of 1.8, 3.2, and 5  $\mu\text{m}$ , respectively. No significant twinning was observed after annealing to suggest modification of the effective grain size. The average grain size is measured on the film surface using ASTM E112. The experiments were carried out in a specially designed tensile micro-fixture fitted to a servoelectric tensile frame (Instron-6642) under displacement control. The fixture has a load cell capacity of 300 N and a noncontact capacitive displacement sensor with 50 nm resolution. The experiments were performed at room temperature at a nominal strain rate of  $2.5 \times 10^{-4} \text{ s}^{-1}$ .

Representative true stress-logarithmic strain curves for different film thickness are shown in Fig. 1 for two sets: 5  $\mu\text{m}$  [Fig. 1(a)] and  $d_g = 1.8 \mu\text{m}$  [Fig. 1(b)]. However, while still quite evident, the thickness-dependent strengthening seen for films with  $d_g = 5 \mu\text{m}$  is not as great as for  $d_g = 1.8 \mu\text{m}$ . When plotting yield stress (at 0.2% strain offset) for all tested samples versus  $1/\sqrt{d_g}$  (Fig. 2), several distinct “near linear” relations can be identified for each film thickness. The correlation slope  $k$  increases with a reduction in

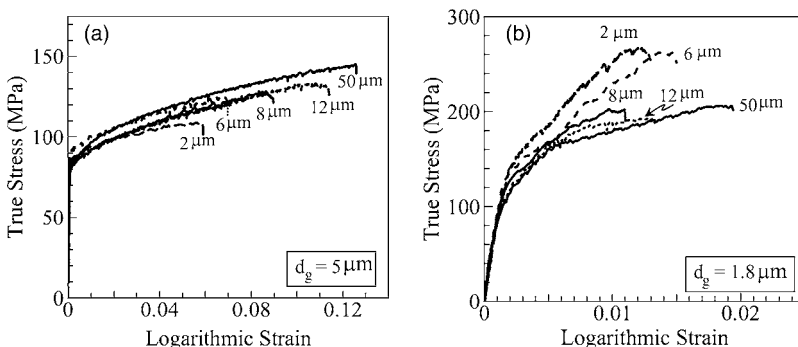


FIG. 1. Typical stress-strain curves for different film thickness for (a)  $d_g = 5 \mu\text{m}$ , showing no variation of the yield strength with film thickness, and (b)  $d_g = 1.8 \mu\text{m}$ , showing a clear increase in film yield strength with a reduction in film thickness.

<sup>a)</sup>Electronic mail: bastaw@iastate.edu.

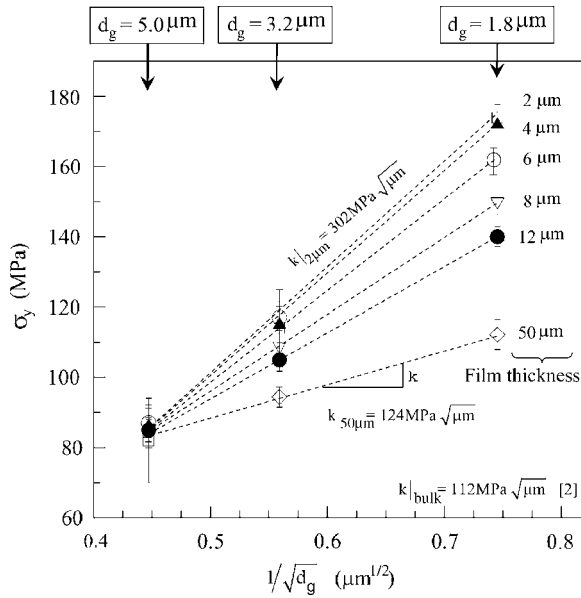


FIG. 2. Variation of yield stress at 0.2% strain offset with  $d_g$  on a Hall-Petch plot for different film thicknesses. The slope of the linear correlations increases with thickness reduction, implying additional thickness-dependent strengthening. The linear correlation for  $t=50 \mu\text{m}$  reaches that of bulk Cu (Ref. 2).

film thickness. The lowest of these correlations for  $t=50 \mu\text{m}$   $k=124 \text{ MPa}\sqrt{\mu\text{m}}$ , which agrees with the bulk Hall-Petch slope for Cu [ $112 \text{ MPa}\sqrt{\mu\text{m}}$  (Ref. 2)]. Figure 2 shows additional film thickness effects beyond the expected grain-size-dependent strengthening for smaller film thicknesses. Moreover, the additional film thickness contribution to strengthening is grain-size dependent, i.e., films with smaller grains ( $1.8 \mu\text{m}$  and  $3.2 \mu\text{m}$ ) are far more sensitive to film thickness reduction than those with larger grains ( $5 \mu\text{m}$ ). Therefore, grain size and thickness effects appear to be coupled on a Hall-Petch plot.

The role of film thickness for a given grain size can be understood as an additional microstructural constraint dependent upon the number of grains across the thickness.<sup>11,12</sup> Such dependence can be clarified by plotting the yield stress versus  $\lambda$  for different  $d_g$  (Fig. 3). For both  $d_g=1.8$  and  $3.2 \mu\text{m}$ , yield strength is found to increase with a reduction in  $\lambda$ . Despite the increase in experimental scatter in the measured strength values with reductions in  $\lambda$ , it is seen, qualitatively speaking, that yield strength retains the same peak level for  $\lambda \leq 1$ , i.e., just one grain across the thickness exposed to the free surface on both sides. However the trend for  $d_g=5 \mu\text{m}$  is quite different, as no thickness-dependent strengthening is observed until a slight weakening trend appears for  $\lambda \leq 1$ . Furthermore, for all cases, the bulk strength predicted by the Hall-Petch relation is attained for large values of  $\lambda \geq 10$ .

Current measurements suggest that the increase in film yield strength observed with the reduction of film thickness at  $d_g=200 \text{ nm}$  (Ref. 3) can be maintained at much larger grain sizes up to about  $5 \mu\text{m}$ , beyond which yield strength becomes independent of film thickness [Fig 1(a)]. Conversely, the strengthening effect becomes more apparent with further reductions in grain size below  $5 \mu\text{m}$ . On the other hand, previous studies<sup>10-12</sup> have shown a weakening effect with reduction in film thickness for grain sizes larger than  $5 \mu\text{m}$ . It is therefore reasonable to assume that  $d_g=5 \mu\text{m}$

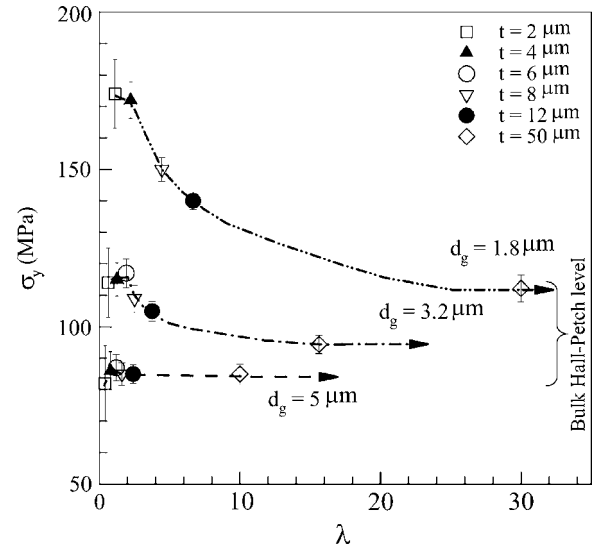


FIG. 3. Variation of yield stress with the number of grains across the film thickness  $\lambda$  for different grain sizes. Thickness-dependent strengthening first emerges at  $d_g=5 \mu\text{m}$  and becomes increasingly prominent with reductions in grain size.

represents a critical grain size threshold  $d_{cr}$ , in which grain-boundary-type (GB-type) dislocation storage and mediated strengthening are nearly balanced by intragranular Frank-Read-type (FR-type) dislocation annihilation at the film-free surface, and mediated weakening.<sup>10,11</sup> At  $d_{cr}$ , two distinct deformation mechanisms, with comparable contributions associated with strengthening as well as weakening, may operate concurrently.

RERM is employed using a standard four-point probe system to identify the underlying deformation mechanisms responsible for  $d_{cr}$  that diminish the observed increase in film yield strength with the reduction of film thickness. Following Mattiessen's rule, the measured resistivity is a collective response of thermal vibrations, impurities, and lattice defects. Lattice defects encompass the bulk resistance due to line defects (dislocation) and point defects (vacancies), as well as the grain boundary resistance. The RERM of nondeformed films at 293 K showed no thickness dependence for each grain size tested. By employing a typical grain boundary resistivity of  $3.6 \times 10^{-4} \mu\Omega \text{ mm}^2$  for copper<sup>13</sup> to account for the volume of averaged grain boundary areas for each grain size, the measurements showed consistent combined line/point defect resistivity of  $0.92 \pm 0.05 \mu\Omega \text{ mm}$ . Such a trend is consistent with various studies of the effects of thickness on the electrical resistivity of Cu films, which show that such effects appear only for 100 nm thickness or less.<sup>14</sup>

The RERM of films deformed at 0.5% strain was also performed. Using constant film processing parameters under quasistatic testing conditions at room temperature, changes in resistivity with strain would indicate accumulated lattice defects as a result of the deformation. As the contribution from vacancy generation can be neglected for tensile loaded films to small strains,<sup>15</sup> the relative change of film resistivity can thus be attributed largely to the generation and storage of dislocations within the intragranular regions as well as at the grain boundaries. Figure 4 shows the relative changes in residual electrical resistivity,  $\bar{\rho}$  (with respect to the undeformed state,  $\rho_0$ ), defined here as  $(\rho_{0.5\%} - \rho_0)/\rho_0$ , of the deformed films as a function of  $t$  for different  $d_g$ . For  $t=50 \mu\text{m}$ , the measured residual resistivity is, generally speaking, inversely

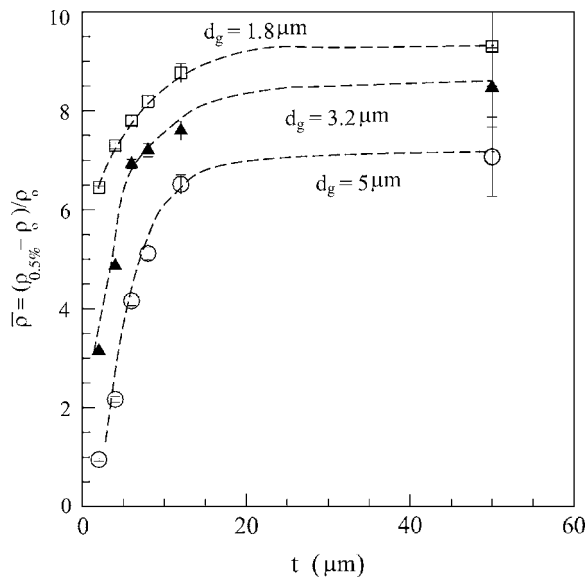


FIG. 4. Variation of film electrical resistivity at 0.5% strain with film thickness. The sharp drop noted for  $d_g=3.5 \mu\text{m}$  and  $d_g=5 \mu\text{m}$  at small thicknesses is attributed to dislocation annihilation at the free surface.

proportional to  $d_g$ , a manifestation of the variation of GB area per unit volume. At smaller film thicknesses,  $\bar{\rho}$  continues to drop, due to the reduction in GB area per unit volume caused by the increase in film surface-to-volume ratio as film thickness is reduced. However, for the two larger grain sizes (viz.,  $d_g=3.5$  and  $5 \mu\text{m}$ ), a sharp drop is seen in the observed trend with reductions in thickness (e.g.,  $\bar{\rho}$  changes significantly for  $d_g=5 \mu\text{m}$  to about 14% of its bulk value for  $\lambda \leq 1$ ). The onset of this sharp drop in the accumulated defect density most likely arises from the annihilation of intragranular FR-type dislocations at the film free surface.

For smaller grains ( $d_g=1.8 \mu\text{m}$ ), there is no sharp drop in  $\bar{\rho}$  with reductions in  $t$ , but instead a rather modest reduction of about 80% in bulk value. This observation can be rationalized if the GBs are the primary source of dislocation at these length scales. Such GB-type dislocations are highly entrapped (or piled up) by the grain boundaries and cannot be annihilated at the free surfaces. Thus, the rather modest reduction observed for  $d_g=1.8 \mu\text{m}$  may be merely the result of reducing GB area by reducing thickness. These measurements may also indicate that a grain size of  $\sim 1.8 \mu\text{m}$  is about the range needed for the dislocation mean free path for FR-type dislocation sources to be active. Preliminary x-ray diffraction measurements performed on the films also provided a qualitative confirmation of the RERM trends observed. Compared to its nondeformed state, the  $d_g=5 \mu\text{m}$  film, strained to 0.5% showed no apparent peak broadening for the  $\langle 111 \rangle$  planes ( $t=4 \mu\text{m}$ ). However, it showed about a fivefold increase in the peak strength. Such an evolution of the diffracting crystalline texture under deformation is possible via the annihilation of substantial intragranular dislocation at the free surface, implying prominent intra-granular dislocation activity in the larger grains. By contrast, a 25% change of the total integrated intensity of the  $\langle 111 \rangle$  peak intensity was observed for  $d_g=1.8 \mu\text{m}$ .

These RERM findings are consistent both with reported dislocation dynamics simulations of deformation mechanisms in fcc materials<sup>8</sup> and with transmission electron microscopy studies,<sup>7,16,17</sup> in which GB dislocations dominate for small grains ( $d_g \sim 50 \text{ nm} - 1 \mu\text{m}$ ). These grain boundary

dislocations are emitted from GB dislocation sources such as GB ledges, after which they traverse the grain and are either absorbed or pileup at the opposite grain boundary.<sup>8,9</sup> The grain interior was shown to be almost dislocation free.<sup>7</sup> In the current study, in which grains are larger than  $1 \mu\text{m}$ , both intragranular as well as GB dislocations are expected to be active.<sup>16</sup> The relative proportion of the two is expected to be mediated by the effective microstructural constraint, including grain size and volume-to-surface-area ratio of the film. In this regard, dislocation dynamics simulations<sup>8</sup> showed that the activation stress for FR-type dislocation sources (i.e., to overcome a critical configuration beyond which dislocation multiplication becomes possible) is sensitive to statistical quantities such as source length and proximity to grain boundaries/free surface. Therefore, a reduction in grain size would reduce the fraction of favorably oriented FR-type dislocation sources and their contribution to overall deformation. It is expected that smaller grains would be significantly affected by GB-type dislocations and increased dislocation storage than larger grains, in which intragranular FR-type dislocations would be more active. In addition, compared to GB-type dislocations, free-surface annihilation would have stronger effects on intragranular dislocation in larger grains.

The film thickness becomes a compounding factor when the GB-type dislocation mechanism is dominating in films with smaller grains ( $1.8$  and  $3.2 \mu\text{m}$ ). Its role can be understood via the change in GB surface area per unit of specimen volume (source density) for a given grain size, rather than the increase in exposure of intragranular volume to free surfaces. At a constant grain size, a reduction in film thickness would reduce the GB surface area per unit of specimen volume, and thereby limits GB dislocation sources. The combined effect leads to strengthening via source starvation.<sup>3</sup> For films with larger grains ( $5 \mu\text{m}$ ), the reduction in effective microstructural constraint by exposure to free surfaces enhances FR-type dislocation mobility and annihilation at free surfaces, thereby minimizing free surface-induced image forces.<sup>7,10,11</sup> Such a free-surface effect would lead to a reduction in strength.

This work is supported by the National Science Foundation under Contract No. CMMI-0134111.

<sup>1</sup>Y. Xiang and J. Vlassak, *Acta Mater.* **54**, 5449 (2006).

<sup>2</sup>D. Y. W. Yu and F. Spaepen, *J. Appl. Phys.* **95**, 2991 (2004).

<sup>3</sup>H. D. Espinosa, B. C. Prorok, and B. Peng, *J. Mech. Phys. Solids* **52**, 667 (2004).

<sup>4</sup>M. A. Haque and M. T. A. Saif, *Acta Mater.* **51**, 3053 (2003).

<sup>5</sup>R. M. Keller, S. P. Baker, and E. Arzt, *J. Mater. Res.* **13**, 1307 (1998).

<sup>6</sup>H. J. Lee, P. Zhang, and J. C. Bravman, *Appl. Phys. Lett.* **84**, 915 (2004).

<sup>7</sup>H. J. Lee, P. Zhang, and J. C. Bravman, *J. Appl. Phys.* **93**, 1443 (2003).

<sup>8</sup>H. D. Espinosa, M. Panico, S. Berbenni, and K. W. Schwarz, *Int. J. Plast.* **22**, 2091 (2006).

<sup>9</sup>V. Yamakov, D. Wolf, S. R. Phillpot, A. K. Mukherjee, and H. Gleiter, *Nat. Mater.* **1**, 45 (2002).

<sup>10</sup>J. S. Stolken and A. G. Evans, *Acta Mater.* **46**, 5109 (1998).

<sup>11</sup>P. J. M. Janssen, Th. H. deKeijser, and M. G. D. Geers, *Mater. Sci. Eng., A* **419**, 238 (2006).

<sup>12</sup>S. Miyazaki, K. Shibata, and H. Fujita, *Acta Metall.* **27**, 855 (1979).

<sup>13</sup>K. M. Mannan and K. R. Karim, *J. Phys. F: Met. Phys.* **5**, 1687 (1975).

<sup>14</sup>J. W. Lim and M. Isshiki, *J. Appl. Phys.* **99**, 094909 (2006).

<sup>15</sup>T. Ungar, E. Schafner, P. Hanak, S. Bernstorff, and M. Zehetbauer, *Mater. Sci. Eng., A* **462**, 398 (2007).

<sup>16</sup>S. Cheng, J. A. Spencer, and W. W. Milligan, *Acta Mater.* **51**, 4505 (2003).

<sup>17</sup>R. R. Keller, J. M. Phelps, and D. T. Read, *Mater. Sci. Eng., A* **214**, 42 (1996).